Evaluating the Relationship Between the Temperature Response to Volcanic Aerosols and Climate Sensitivity

by

Warittha Panasawatwong

Submitted to the Department of Earth, Atmospheric and Planetary Sciences

in Partial Fulfillment of the Requirements for the Degree of

Bachelor of Science in Earth, Atmospheric and Planetary Sciences

at the Massachusetts Institute of Technology

May 25, 2017 [June 2017]

Author Signature redacted

Department of Earth, Atmospheric and Planetary Sciences
May 25, 2017

Certified by Signature redacted

Paul O'Gorman
Thesis Supervisor

Accepted by Signature redacted

Richard P. Binzel
Chair, Committee on Undergraduate Program

Evaluating the Relationship Between the Temperature Response to Volcanic Aerosols and Climate Sensitivity

by

Warittha Panasawatwong

Submitted to the Department of Earth, Atmospheric and Planetary Sciences

in Partial Fulfillment of the Requirements for the Degree of

Bachelor of Science in Earth, Atmospheric and Planetary Sciences

Abstract

Climate sensitivity is an important concept in climate science, but its estimated value has considerable uncertainty. Some previous studies have argued for a link between the temperature response to volcanic radiative forcing and climate sensitivity. Bender et al. (2010) showed that equilibrium climate sensitivity is correlated across Coupled Model Intercomparison Project Phase 3 (CMIP3) models to the ratio of surface temperature response to top-of-atmosphere shortwave radiation response following Pinatubo, when excluding one anomalous model. In this thesis, Bender et al.'s calculation for CMIP3 models was repeated and was found to give a correlation coefficient of -0.44 ($p = 0.23$), which is lower than what Bender et al. found. Extension to Coupled Model Intercomparison Project Phase 5 (CMIP5) models also shows a lower correlation coefficient. Using transient climate response instead of equilibrium climate sensitivity or lower-troposphere temperature instead of surface air temperature in Bender et al.'s approach increased the correlation coefficient. Alternatively, regression of the temperature response on the shortwave radiative response and an ENSO index gave the highest correlation with climate sensitivity for a 7-year running mean surface temperature series ($r = -0.65$, $p = 0.04$) and a 7-year running mean lower-troposphere temperature series ($r = -0.68$, $p = 0.03$) based on CMIP5 models. Future work could explore the use of a transient climate response calculated from lower-troposphere temperature or a transient climate response of even shorter time-scale as alternative measures of climate sensitivity.

Thesis adviser: Paul O'Gorman
Title: Associate Professor

Acknowledgement

I would like to thank you Prof. Paul O'Gorman. I am very grateful for his help and advice throughout this thesis project. He always goes above and beyond regarding the direction of the project.

I would like to thank Prof. Frida Bender, who helped me reproducing the result in her paper.

I would like to thank Jane O'Connor for support and help in writing this thesis.

And thanks to the MIT Undergraduate Research Opportunities Program for funding this project during summer 2016.

Contents

List of Figures

List of Tables

Chapter 1

Introduction

Volcanic aerosols are an important radiative forcing. Sulfuric gasses from large volcanic eruptions enter the stratosphere, where they are oxidized and form sulfate aerosol haze. The haze can spread throughout the globe. The sulfate aerosols reflect incoming shortwave and increase the planet's albedo, resulting in a global short-term cooling effect over 1-5 years (Rampino, 1984). The aerosol's short timescale makes it easy to observe the temperature response to the forcing. Moreover, in one-dimensional models, global mean temperature responds similarly to the magnitude of different radiative forcings (IPCC, 2001). Volcanic aerosols are a good natural forcing to study the degree to which the climate system may respond to other forcings (Soden et al, 2002). One of most interesting radiative forcing agents is CO_2, a significant greenhouse gas.

Greenhouse gasses act as a radiative forcing that absorbs longwave radiation and in turn, traps heat within earth's atmosphere. The large emissions of CO_2 make CO_2 the most significant anthropogenic greenhouse gas. A measure used to represent how much the temperature responds to CO_2 forcing is equilibrium climate sensitivity ($\Delta T_{2\times CO_2}$), defined as the change of global mean surface air temperature in response to an instantaneous doubling of CO_2 in the atmosphere after the temperature has reached equilibrium. Another measure is transient climate response (TCR), defined as the global mean surface air temperature change when CO_2 is increased by 1% per year at the time of doubling of CO_2. Even though equilibrium climate sensitivity is a more popular measure, TCR's shorter time scale makes it more suitable for predicting near-future global temperature. These two measures can be computed using global climate models' (GCMs) experiments on instantaneous and incremental CO_2 doubling. IPCC (2013) reports Coupled Model Intercomparison Project Phase 5 (CMIP5) GCMs' range of $\Delta T_{2\times CO_2}$ of 3.2 ± 1.3 K and TCR of 1.8 ± 0.6 K with 90% uncertainty.

Volcanic radiative forcing is a good candidate for an observational constraint in estimating climate sensitivity. By drawing a correlation between GCMs' volcanic

temperature response and climate sensitivity. the earth's climate sensitivity can be estimated from the observed volcanic temperature response. Several studies have shown higher climate sensitivity correlates with stronger temperature response to volcano radiative forcing (Lindzen and Giannitsis, 1998, Wigley et al, 2005a, Yokohata et al, 2005), even though the resulting estimated range of earth's climate sensitivity is varied.

There is evidence in the literature that the volcanic temperature response and radiative forcing in GCMs alone are not enough to infer climate sensitivity, because of the influence of the heat flux from the ocean mixed layer into the deep ocean (Boer et al., 2007, Wigley et al, 2005b). After a volcanic eruption, volcanic aerosols reflect incoming radiation and this has an immediate cooling effect on the atmosphere temperature and rapidly decreases the ocean heat content (Church et al., 2005). Ocean heat flux between the cooled ocean and the atmosphere prolongs the volcanic forcing's cooling effect on the atmosphere. CMIP5 models are atmosphere-ocean coupled models with representations of the ocean mixed-layer and deep ocean. To the extent that each model simulates the heat flux into the ocean correctly, we can still expect a correlation between climate sensitivity and temperature and radiative perturbation over the same span of time.

Bender et al. (2010) uses two constraints: temperature and radiative perturbation following a volcanic eruption, to estimate climate sensitivity, using Coupled Model Intercomparison Project Phase 3 (CMIP3) simulations and focusing on the eruption of Mt. Pinatubo in 1991. Even though several models use the same aerosol optical depth series as their volcanic parameterization, it leads to different radiative forcing in different models. However, volcanic radiative forcing cannot be easily observed or calculated in the model. The radiative perturbation in top-of-atmosphere reflected shortwave is used as an index of volcanic radiative forcing. After subtracting the seasonal cycle and de-trending the data, temperature and shortwave anomalies are integrated over a period of time following the Pinatubo eruption. The result fails to show a significant correlation between integrated temperature perturbation and climate sensitivity. While integrated radiative response to volcanic aerosols has significant correlation with climate sensitivity, it can be explained that the aerosol optical depth was tuned to give temperature responses that match observations, regardless of climate sensitivity. However, the scaled temperature

perturbation, calculated as a ratio of integrated temperature perturbation and integrated shortwave, shows a linear relation to climate sensitivity with a correlation of -0.80 that is 95% significant when excluding one anomalous model. The emergent linear relationship is used to estimated climate sensitivity using the observed radiative flux from the Earth Radiation Budget Experiment (ERBE) and the temperature response from ERA40. The estimated climate sensitivity is between 1.7 K and 3.2 K.

To study the robustness of the scaled temperature perturbation method, this thesis extends the data set onto CMIP5 models. Moreover, Foster and Rahmstorf (2011) suggests that lower-troposphere temperature (TLT) responds more strongly to volcanic forcing than surface air temperature (TAS), and with a higher signal to noise, so we experimented with using scaled TLT perturbation as well. We also experimented with different climate sensitivities, using TCR as a measure of the shorter-timescale temperature response. TCR is a measure of climate sensitivity that is more practical for policy making.

By using a regression method, following Foster and Rahmstorf (2011), more than one volcanic event can be easily included. Integrated temperature time series can be made to take account of ocean heat storage by integrating elements in a specified time span to give one element in the integrated time series (i.e. by taking a running mean over a certain number of years). The regression approach also allows the removal of the influence of ENSO by using an ENSO index as a regression predictor. In this thesis, the nino 3.4 index is used as a regression predictor for ENSO, and the reflected shortwave perturbation is used as volcanic forcing's regression predictor.

Chapter 2 of this thesis presents the model data used for analysis. Chapter 3 presents results from using Bender et al.'s method with CMIP5 TAS and TLT and an effort to reproduce Bender et al.'s results for CMIP3 TAS. Chapter 4 presents results using the regression approach for CMIP3 TAS and in CMIP5 TAS and TLT. The discussion and conclusion are in chapter 5.

Chapter 2

Models and data

CMIP3 models were used to perform simulations for the twentieth century climate, including forcings from anthopogenic greenhouse gases, atmospheric aerosols, solar variability, etc. However, only twelve models included volcanic forcing. Two models, MRI-CGCM2.3.2 and ECHO-G, which parameterized volcanic forcing through solar constant modification are not included in the analysis, because the reflected shortwave would not contain any perturbation response. The remaining ten models parameterize volcanic forcing through modification of aerosol optical depth at 550 nm as estimated by Sato et al. (1993) or Ammann et al. (2007) (see Table 1). The required variables are obtained from the World Climate Research Program portal (https://esgf-node.llnl.gov /search/cmip3). Even though most models have at least three realizations, MIROC3.2 (hires), INM-CM3.0, and UKMO-HadGEM1 only have one realization. For models that have at least three realization, the temperature and reflected shortwave series are averaged into ensemble-mean time series to reduce noise.

CMIP5 models were used to perform historical simulation including forcings from atmospheric composition, solar variations, emissions of natural and anthropogenic aerosols or their precursors, etc. according to available historical data. Unlike in CMIP3, all the models include volcanic forcing. Lower-troposphere temperature time series used in this thesis are only obtained from CMIP5 models. The weighting function for calculating lower-troposphere temperature was obtained from Remote Sensing Systems (http://www.remss.com/measurements/upper-air-temperature#zonal_anomalies). The required variables were obtained from the World Climate Research Program portal (https://esgf-node.llnl.gov/search/cmip5). From all CMIP5 models, only ten available models have at least 3 realizations in the historical experiment with volcanic radiative forcing present in reflected shortwave radiation and transient climate response available. These models are used here and their ensemble-mean temperature and reflected shortwave time series are computed to reduce noise. However, different models may use volcanic parameterizations from Sato et al. (1993) or Ammann et al. (2003) (see Table 2).

Table 2.1. CMIP3 models used in estimating climate sensitivity (adapted from Bender et al. (2010))

Model name	Atmospheric resolution	Volcanic parameterization
GFDL CM2.0 (OM3P4)	2.0° × 2.5° L24	Sato et al. (1993)
GFDL CM2.1 (OM3P4)	2.0° × 2.5° L24	Sato et al. (1993)
GISS-EH (HYCOM)	4.0° × 5.0° L20	Ammann et al. (2007)
GISS-ER (Russell)	4.0° × 5.0° L20	Sato et al. (1993)
PCM (POP)	T42 L26	Ammann et al. (2007)
MIROC3.2 (medres)	T42 L20	Sato et al. (1993)
MIROC3.2 (hires) (COCO3.3)	T106 L56	Sato et al. (1993)
INM-CM3.0	4.0° × 5.0° L21	Ammann et al. (2007)
UKMO-HadGEM1	N96 L38	Sato et al. (1993)
CCSM3 (POP 1.4.3)	T85 L26	Ammann et al. (2007)

Table 2.2. CMIP5 models used in this study

Model name	Atmospheric resolution	Volcanic parameterization
ACCESS1.0	1.251.875° N96	
ACCESS1.3	1.25° × 1.875° N96	
CNRM-CM5	1.40080° ×1.40625° T127 L31	Ammann et al. (2007)
GFDL-CM3	2.0° × 2.5° C48 L48	Sato et al. (1993)
GISS-E2-H	2.0° × 2.5° L40	Sato et al. (1993)
GISS-E2-R	2.0° × 2.5° L40	Sato et al. (1993)
MIROC-ESM	2.7906° × 2.8125° T42 L80	Sato et al. (1993)
MIROC5	1.4008° × 1.40625° T85 L40	Sato et al. (1993)
MPI-ESM-LR	1.8653° × 1.8750° T63 L47	Sato et al. (1993)
MPI-ESM-MR	1.8653° × 1.8750° T63 L47	Sato et al. (1993)

The equilibrium climate sensitivity of CMIP3 models used in this thesis was obtained from Bender (2010). The equilibrium climate sensitivity and transient climate response of CMIP5 models used in this thesis was obtained from the IPCC fifth assessment report (2013).

To reproduce and extend the scaled temperature perturbation method, the same method used in Bender et al. (2010) is applied to surface air temperature and reflected shortwave radiation time series from CMIP3 and CMIP5 models. The time series were de-seasonalized by subtracting the 1985 – 1990 mean for each calendar month, which is the period after the surface temperature and radiation response to the eruption of El Chichón in April 1982 has decayed back to the equilibrium and preceding the eruption of Pinatubo in June 1991. Linear trends in the temperature anomalies from the studied period 1985 – 2000 are then removed.

For the regression analysis, all temperature and radiative time series are restricted to the time length of 1951-2005 and de-seasonalized by subtracting the 1951-2005 mean, which is the period over which all model data overlaps. Nino 3.4 time series are computed from surface temperature anomalies as the ENSO index for each model.

Chapter 3

Results: Bender et al.'s approach in CMIP3 and CMIP5

3.1 Reproducing result from Bender et al. (2010) for CMIP3

The surface temperature anomalies from ten CMIP3 models are plotted in figure 3-1, and the tropical (20°N – 20°S) top-of-atmosphere reflected shortwave anomalies are plotted in figure 3-2. The tropical-mean shortwave is used instead of the global-mean shortwave because the global-mean series show a 25% smaller peak compared with the tropical-mean series (Bender et al, 2010).

The scaled temperature perturbation for each model is then calculated using the same method described in Bender et al. (2010). The scaled temperature perturbation is calculated as the ratio of the integrated temperature perturbation from June 1991 to June 1995 to the integrated shortwave perturbation from June 1991 to June 1993. Bender found the scaled temperature response to be a good emergent constraint for estimating equilibrium climate sensitivity, with correlation coefficient of -0.80 (95% significant), when excluding INM-CM3.0 as an outlier. Bender et al.'s (2010) result is shown in figure 3-3.

The current study could partially reproduce Bender et al.'s result, with the ratios from five of ten models agreeing with the original ratios, shown in figure 3-4. It is unclear why we were unable to exactly reproduce the original results. It is possible that some of the data changed, and unfortunately the errata page for CMIP3 model output was not available at the time of this study. We assume that the level of agreement is good enough to warrant proceeding to CMIP5. However, our calculation for CMIP3 produced a correlation coefficient of only -0.44 with a p-value of 0.23.

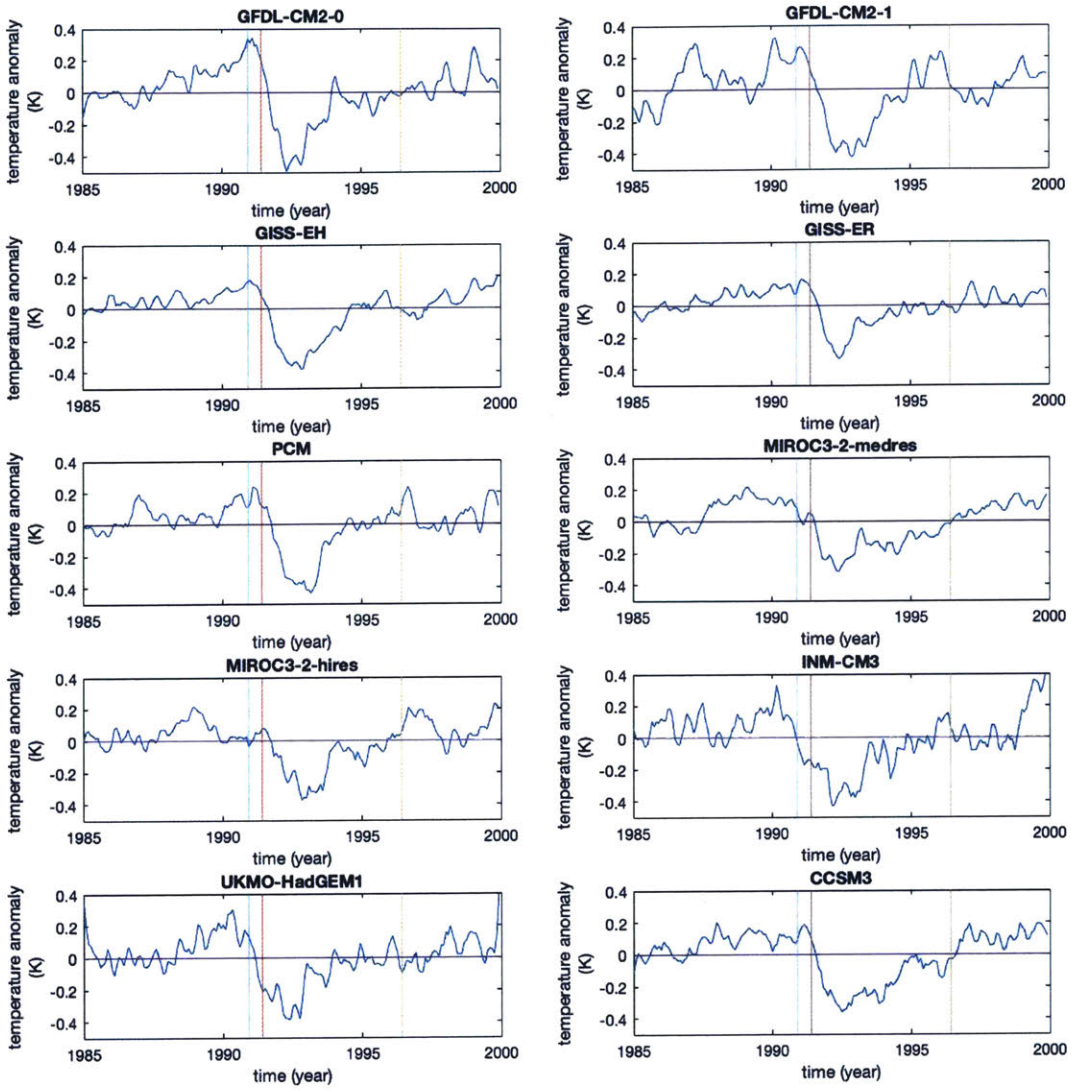

Figure 3-1. Global mean, monthly mean surface air temperature anomalies from CMIP3 models. The vertical lines show the period that the seasonal cycle is calculated (1985-1990) and the period that the integrated temperature perturbations are calculated (June 1991– June 1995). The time series are displayed smoothed with a 3-month running mean.

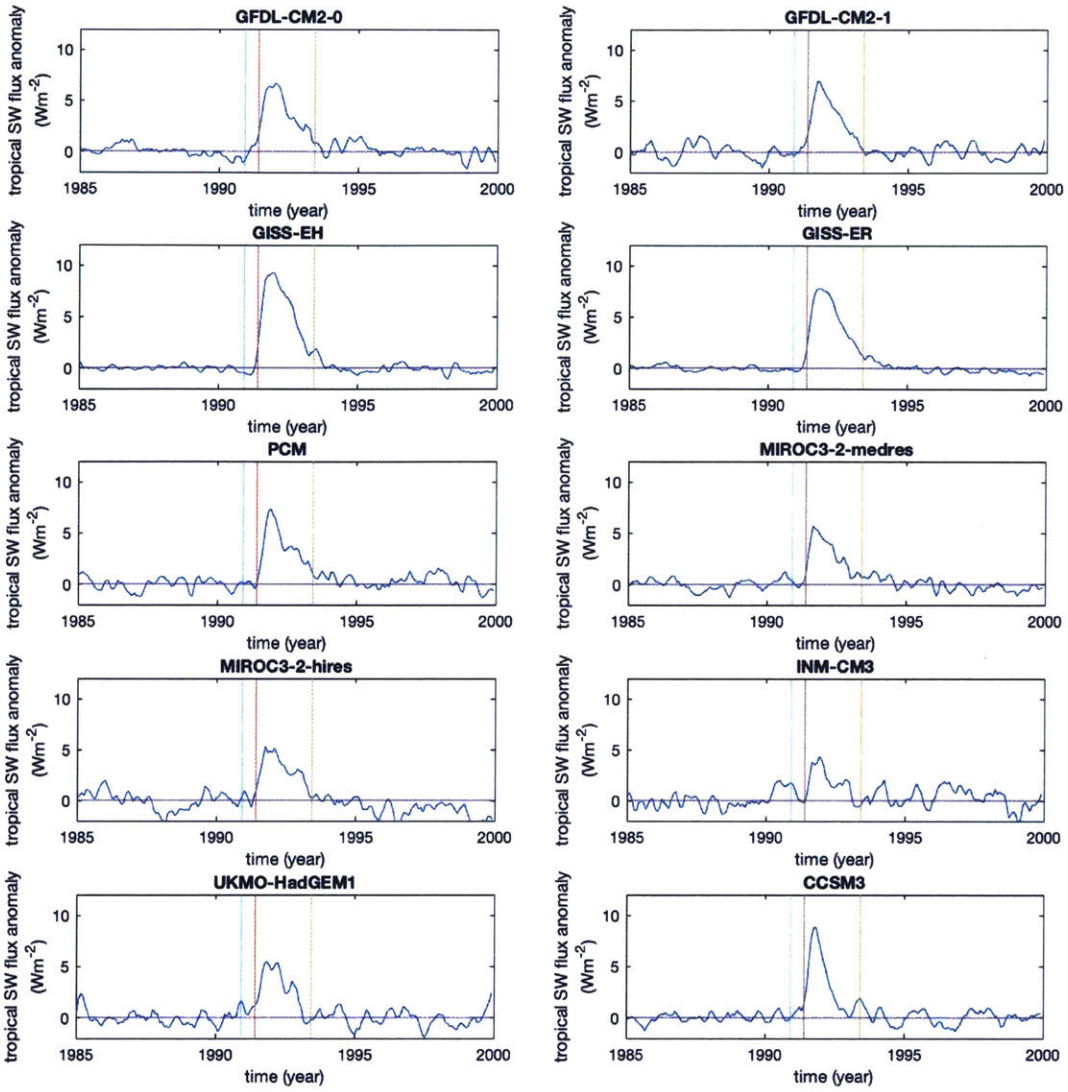

Figure 3-2. Tropical (20°N – 20°S) mean, monthly mean reflected shortwave anomalies from CMIP3 models. The vertical lines show the period that the seasonal cycle is calculated (1985-1990) and the period that the integrated temperature perturbations are calculated (June 1991– June 1993). The time series are displayed smoothed with a 3-month running mean.

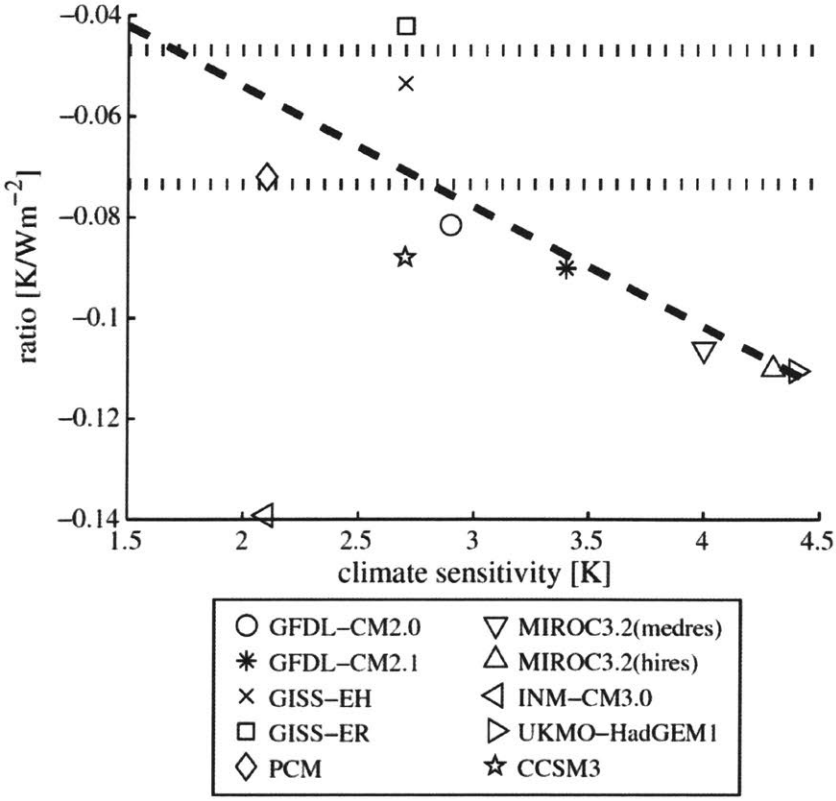

Figure 3-3. Ratio of integrated surface temperature anomaly (June 1991 - June 1995) and integrated tropical shortwave anomaly (June 1991 - June 1993), plotted against equilibrium climate sensitivity. The dash line shows the best fit line of the data after excluding INM-CM3.0 anomalous result. The horizontal dotted lines indicate the range of the ratio calculated from observations. The correlation coefficient across models is -0.80 which is 95% significant. (From Bender et al, 2010 with permission)

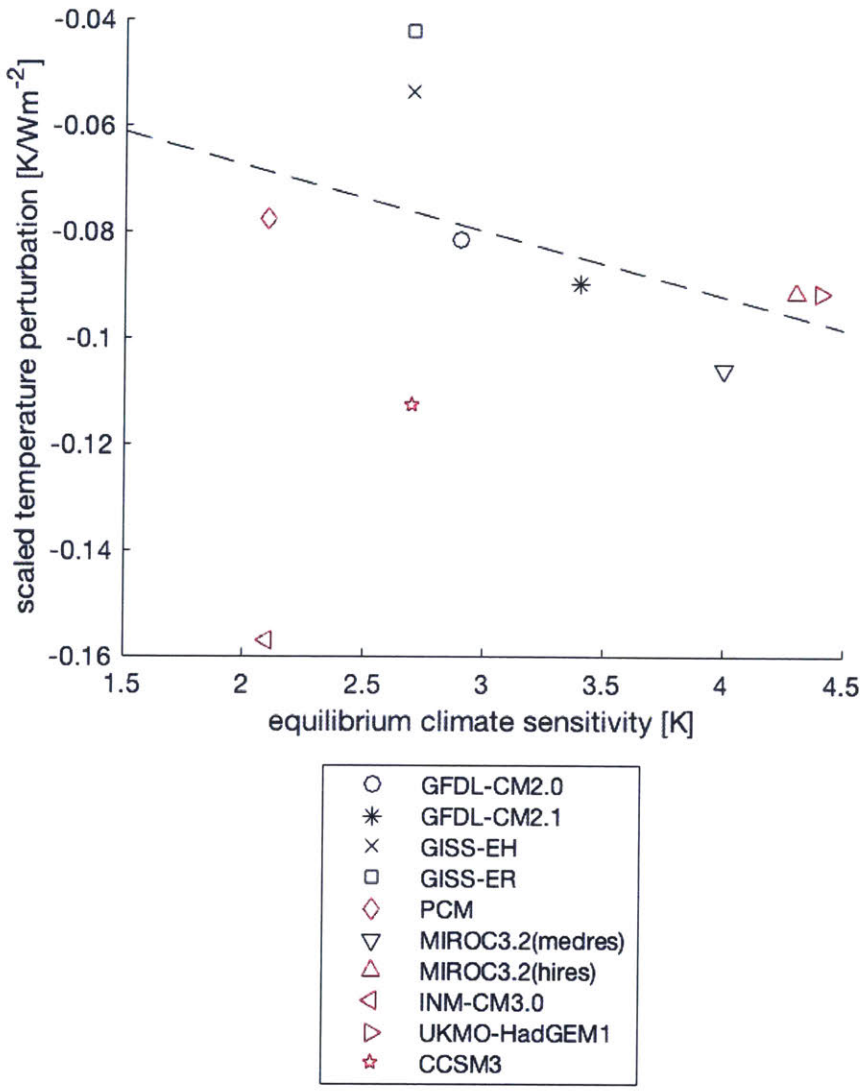

Figure 3-4. Scaled temperature perturbation, or ratio of integrated surface temperature anomaly (June 1991 - June 1995) and integrated tropical shortwave anomaly (June 1991 - June 1993), plotted against equilibrium climate sensitivity of CMIP3 models, in an attempt to reproduce the Bender et al. (2010) result. Black markers show calculations that agree with the original results in Bender (2010, and red markers show calculations that do not agree. The dashed line shows the best fit line of this data set, excluding INM-CM3.0 anomaly. The correlation coefficient is -0.44 with $p = 0.23$.

3.2 Extending Bender et al.'s approach to CMIP 5

The surface temperature anomalies from ten CMIP5 models are plotted in figure 3-5, and the tropical (20°N – 20°S) top-of-atmosphere reflected shortwave anomalies are plotted in figure 3-6. The scaled temperature perturbation for each model is then calculated using the same Bender et al.'s approach as described in section in 3.1. However, only eight of ten models have a value for the equilibrium climate sensitivity reported in IPCC (2013). Figure 3-7 shows the scaled surface temperature perturbation versus ECS. The result shows a weak correlation of -0.22 with $p = 0.60$, so there is no significant correlation between the scaled surface temperature perturbation and equilibrium climate sensitivity in CMIP5

3.3 Bender et al.'s Approach using transient climate response

Transient climate response (TCR) has a timescale of 70 years, while equilibrium climate sensitivity (ECS) has timescale of order 500 years. The temperature response to volcanic forcing has time scale of order 5 years. Therefore, TCR's timescale is closer to the volcanic forcing's than ECS's, and so TCR should correlated better with the temperature response to volcanic forcing better than ECS. Figure 3-8 shows the scaled surface temperature perturbation versus TCR. This yields a correlation coefficient of -0.38 with $p = 0.28$. Compared with the equilibrium climate sensitivity, TCR produces a larger correlation coefficient. However, the improvement is relatively small and the correlation is still not significant.

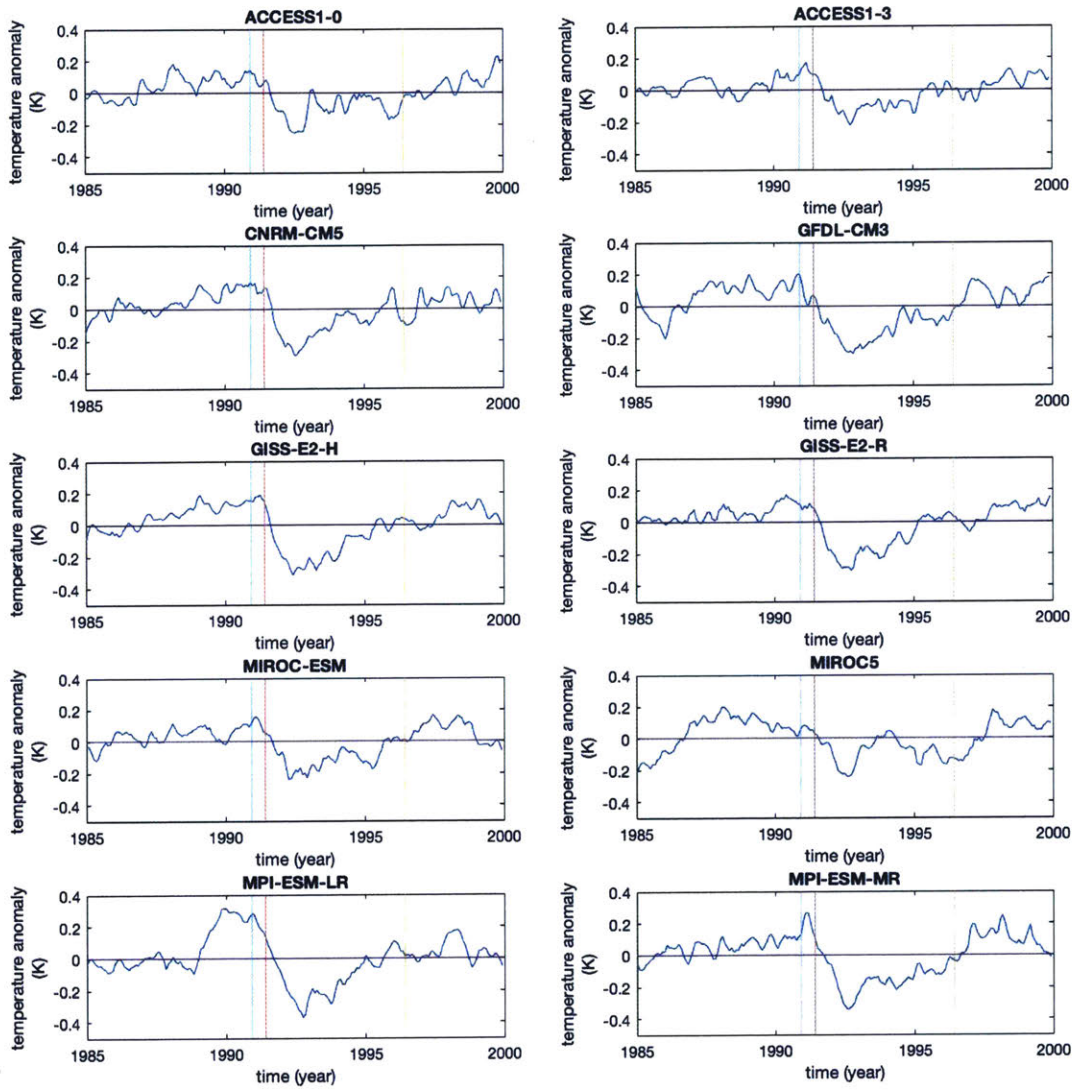

Figure 3-5. Global mean, monthly mean surface air temperature anomalies from CMIP5 models. The vertical lines show the period that the seasonal cycle is calculated (1985-1990) and the period that the integrated temperature perturbations are calculated (June 1991– June 1995). The time series are displayed smoothed with a 3-month running mean.

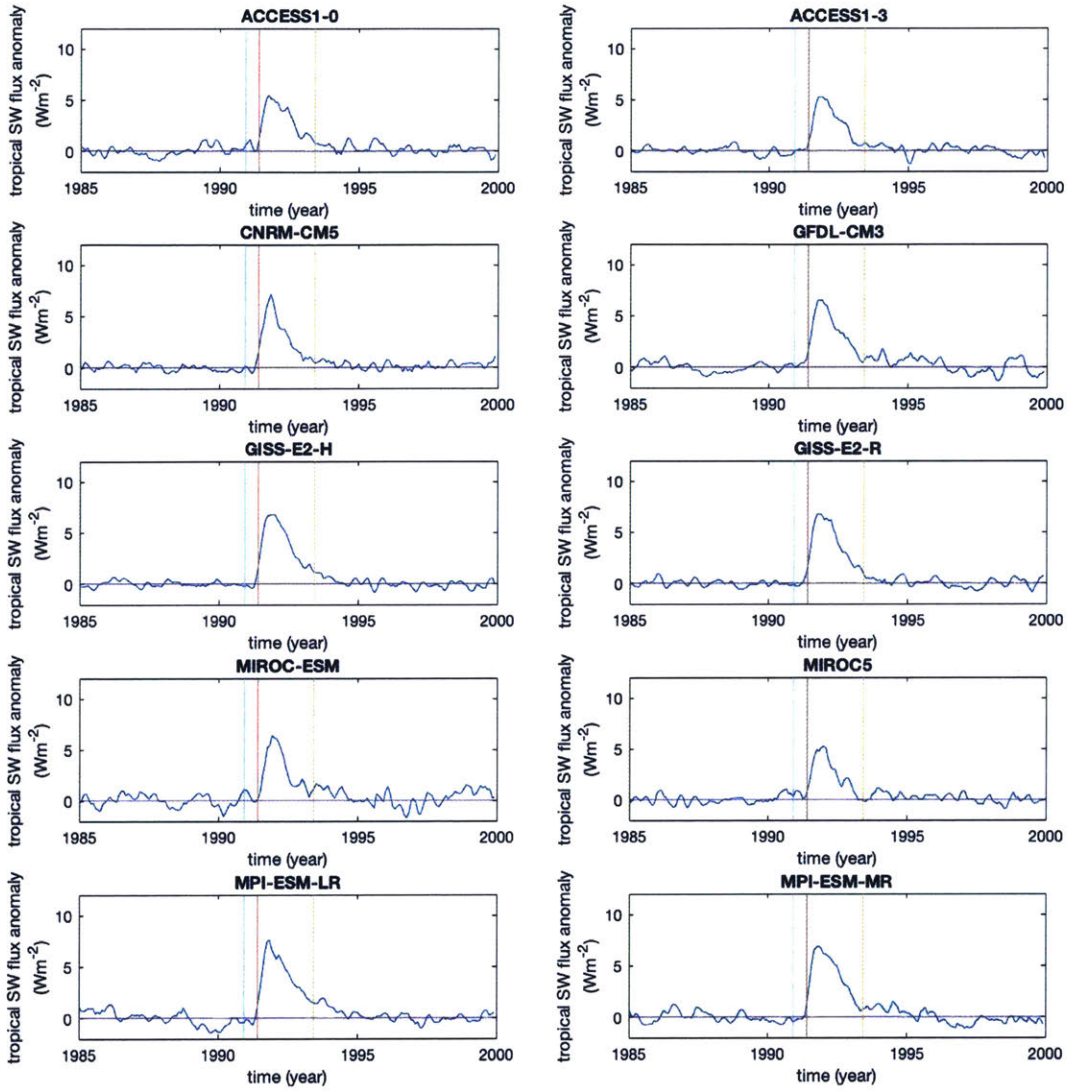

Figure 3-6. Tropical (20°N – 20°S) mean, monthly mean reflected shortwave anomalies from CMIP5 models. The vertical lines show the period that the seasonal cycle are calculated (1985-1990) and the period that the integrated temperature perturbations are calculated (June 1991– June 1993). The time series are displayed smoothed with a 3-month running mean.

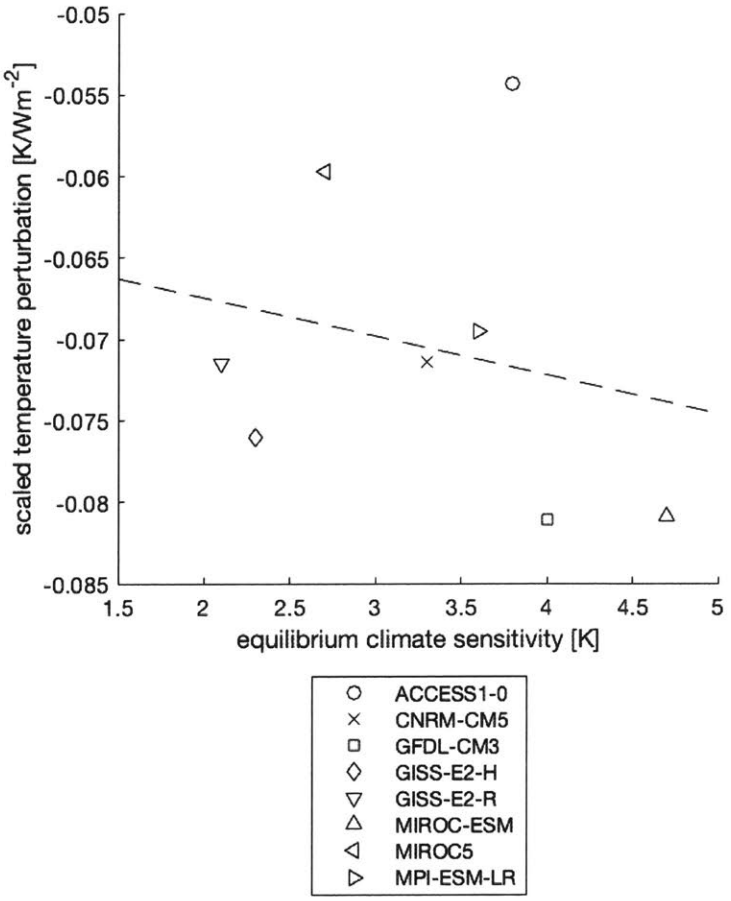

Figure 3-7. Scaled temperature perturbation, or ratio of integrated surface temperature anomaly (June 1991 - June 1995) and integrated tropical shortwave anomaly (June 1991 - June 1993), plotted against equilibrium climate sensitivity of CMIP5 models. The dashed line shows the best fit line of this data set. The correlation coefficient is of -0.22 with p = 0.63.

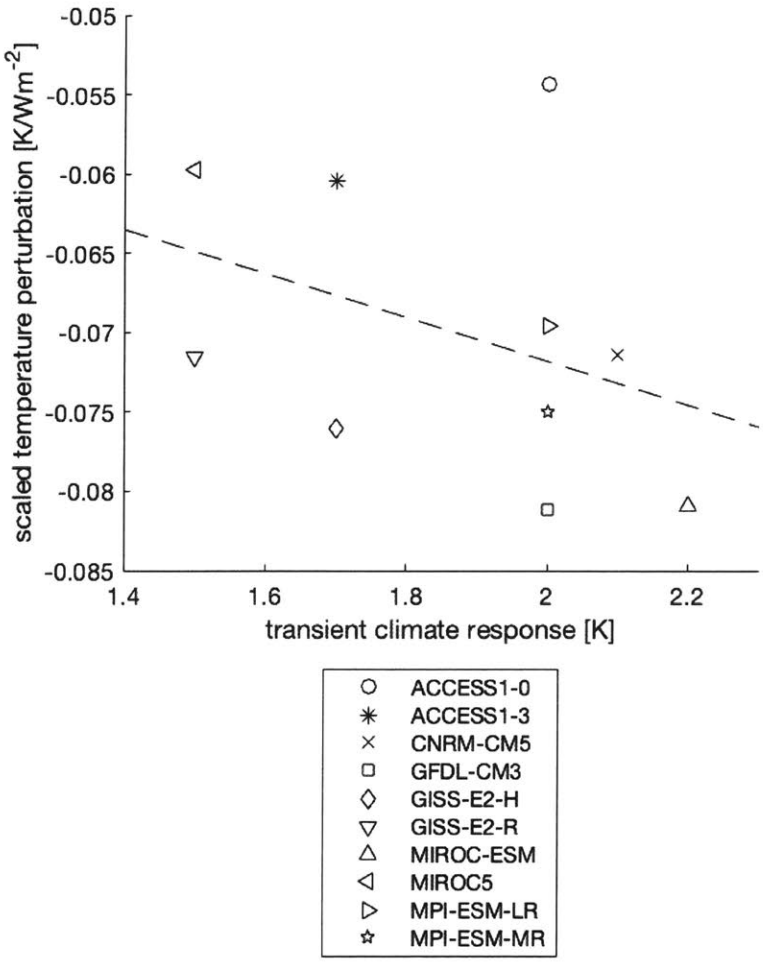

Figure 3-8. Scaled surface temperature perturbation, or ratio of integrated surface temperature anomaly (June 1991 - June 1995) and integrated tropical shortwave anomaly (June 1991 - June 1993), plotted against transient climate response (TCR). The dashed line shows the best fit line of this data set. The correlation coefficient is -0.38 with $p = 0.28$.

3.4 Bender et al.'s Approach using lower-troposphere temperature

Foster and Rahmstorf (2011) showed that lower troposphere temperature (TLT) is more responsive to volcanic forcing than surface air temperature (TAS) (figure 3-9). TLT has a larger regression coefficient to aerosol optical depth (AOD) than TAS, but still has a similar range of uncertainty. Thus, the TLT response to volcanic aerosols shows potential as a stronger constraint for climate sensitivity than TAS. Global mean TLT series are shown in figure 3-10.

The scaled temperature response calculated from TLT shows slightly stronger correlation to both equilibrium climate sensitivity (figure 3-11) with $r = -0.43$, $p = 0.29$ and transient climate response (figure 3-12) with $r = -0.40$, $p = 0.25$. However, these correlation coefficients are still not statistically significant.

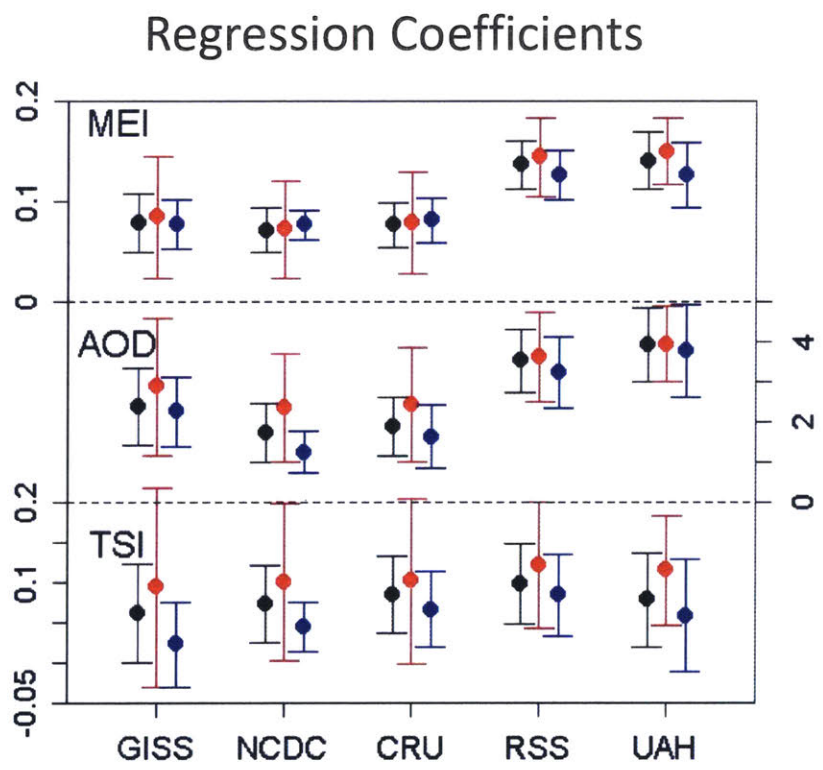

Figure 3-9. Regression coefficients of observed surface temperature response (GISS, NCDC, and CRU) and lower-troposphere temperature response (RSS and UAH) to multivariate el Niño index (MEI), aerosol optical depth (AOD) and total solar irradiance (TSI). AOD is also used as a volcanic aerosol forcing index. Lower-troposphere temperature response has a stronger signal to noise ratio for volcanic aerosols. (From Forster and Rahmstorf, 2011; Published under a Creative Commons license)

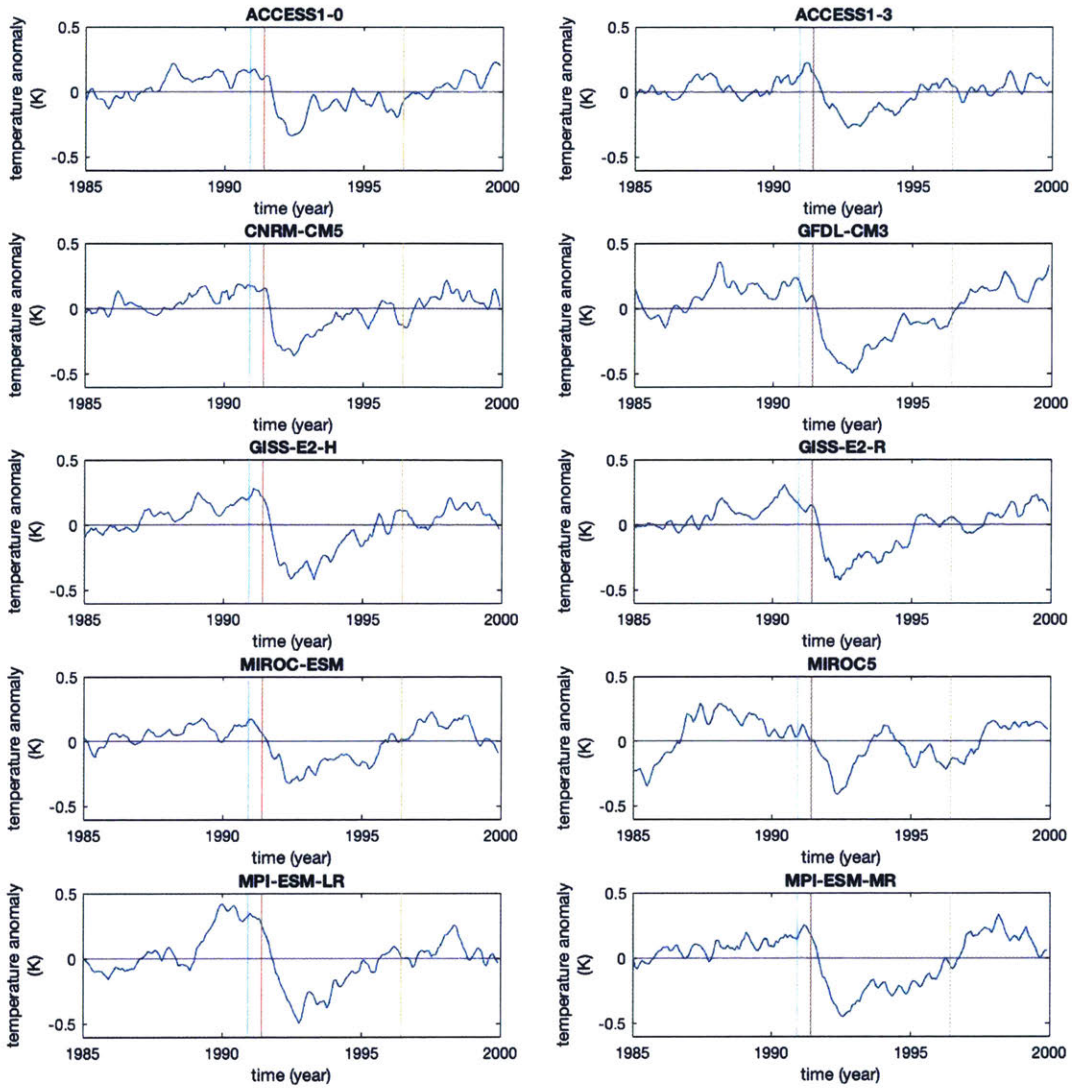

Figure 3-10. Global mean, monthly mean lower-troposphere temperature anomalies from CMIP5 models. The vertical lines show the period over which the seasonal cycle is calculated (1985-1990) and the period over which the integrated temperature perturbations are calculated (June 1991– June 1995). The time series are displayed smoothed with a 3-month running mean.

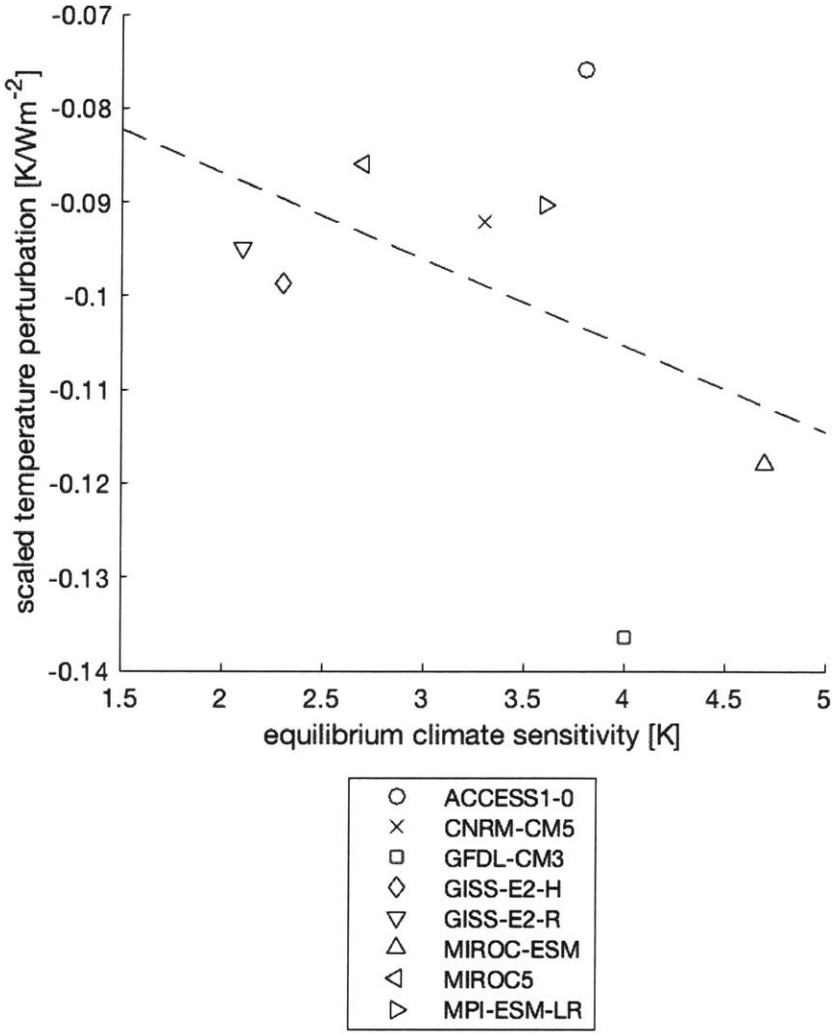

Figure 3-11. Scaled temperature perturbation using integrated lower-troposphere temperature anomaly (from June 1991 - June 1995 mean) and integrated tropical shortwave anomaly (June 1991 - June 1993), plotted against equilibrium climate sensitivity. The dashed line shows the best fit line of this data set. The correlation coefficient is -0.43 with p = 0.29.

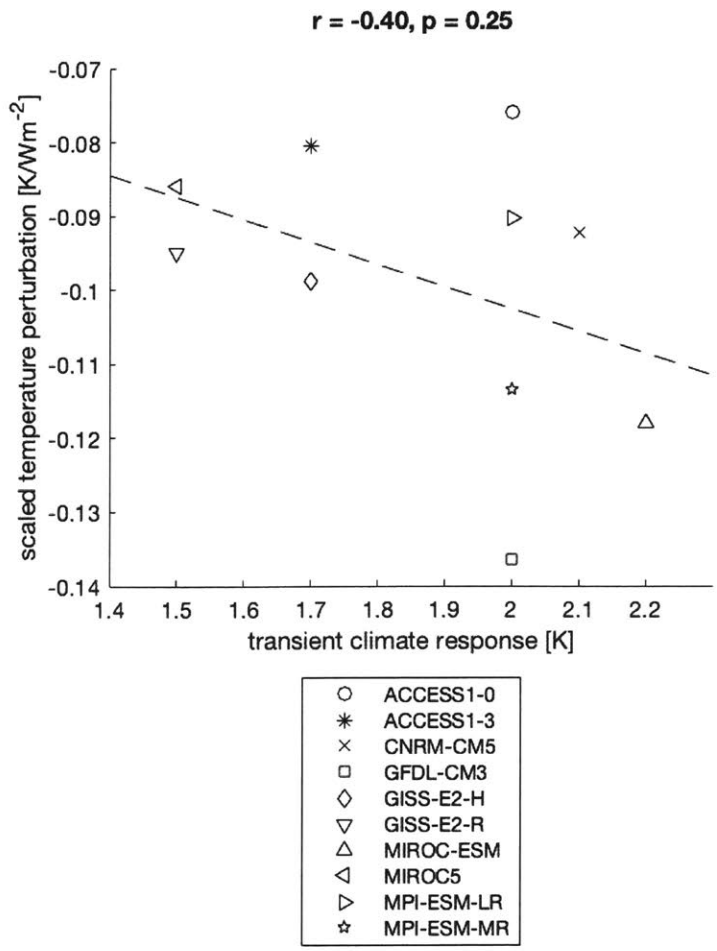

Figure 3-12. Scaled temperature perturbation using integrated lower-troposphere temperature anomaly (from June 1991 - June 1995 mean) and integrated tropical shortwave anomaly (June 1991 - June 1993), plotted against transient climate response. The dashed line shows the best fit line of this data set. The correlation coefficient is -0.40 with p = 0.25.

Chapter 4

Results: Regression Approach

Foster and Rahmstorf (2011) used multiple linear regression to analyze the influence of different factors on TAS and TLT with specified lag for each factor (figure 3-9). However, the lagged temperature response to the forcings alone may not be enough to constrain climate sensitivity due to the heat flux into the ocean (Boer et al., 2007, Wigley et al, 2005b). Integrating the temperature series over time may better account for the influence from the ocean while minimizing the influence of noise. Boer et al. (2007) suggested that averaging temperature series over 8 – 10 years is the most suitable. In our approach, the temperature time series is averaged with a 3 to 10 – year running mean. Multiple regression was then performed on the running-mean temperature series against other factors (evaluated at the start of the running mean), with reflected shortwave as the volcanic forcing index, nino 3.4 as the ENSO index, and the time vector as an additional factor to account for the long-term warming trend.

Advantages of the regression approach over the Bender et al.'s approach are that the regression approach allows for subtraction of ENSO influence from the volcanic response signal by using an ENSO index in the multiple regression. The regression approach also allows for longer series to be included in the calculation than in Bender et al.'s approach, accounting for more than one eruption.

Figure 4-1 shows the plot of 7-year running mean TAS series for CMIP5 models. After each running meaning series was computed, the regression was run. The correlation between the regression coefficient of temperature response to volcanic forcing and the model's respective transient climate response was computed for each running mean temperature series, and the correlation coefficient is plotted in figure 4-2 as a function of averaging time. The maximum correlation was yielded from the 7-year running mean series. The scatter plot of the 7-year running mean series' regression coefficient of temperature response to volcanic forcing versus transient climate response for different models is plotted in figure 4-3. The correlation coefficient of -0.65 with $p = 0.04$.

The same method was applied to the CMIP5 TLT series. Figure 4-4 shows 7-year running mean TLT series. The correlation coefficient between TLT's regression coefficient and the transient climate response, showed in figure 4-5, is most negative when TLT is averaged with a 7–year running mean. Figure 4-6 shows a scatter plot of CMIP5 TLT regression coefficient versus TCR for this running mean time. The correlation coefficient is 0.68 with p = 0.03, slightly better than the correlation from TAS.

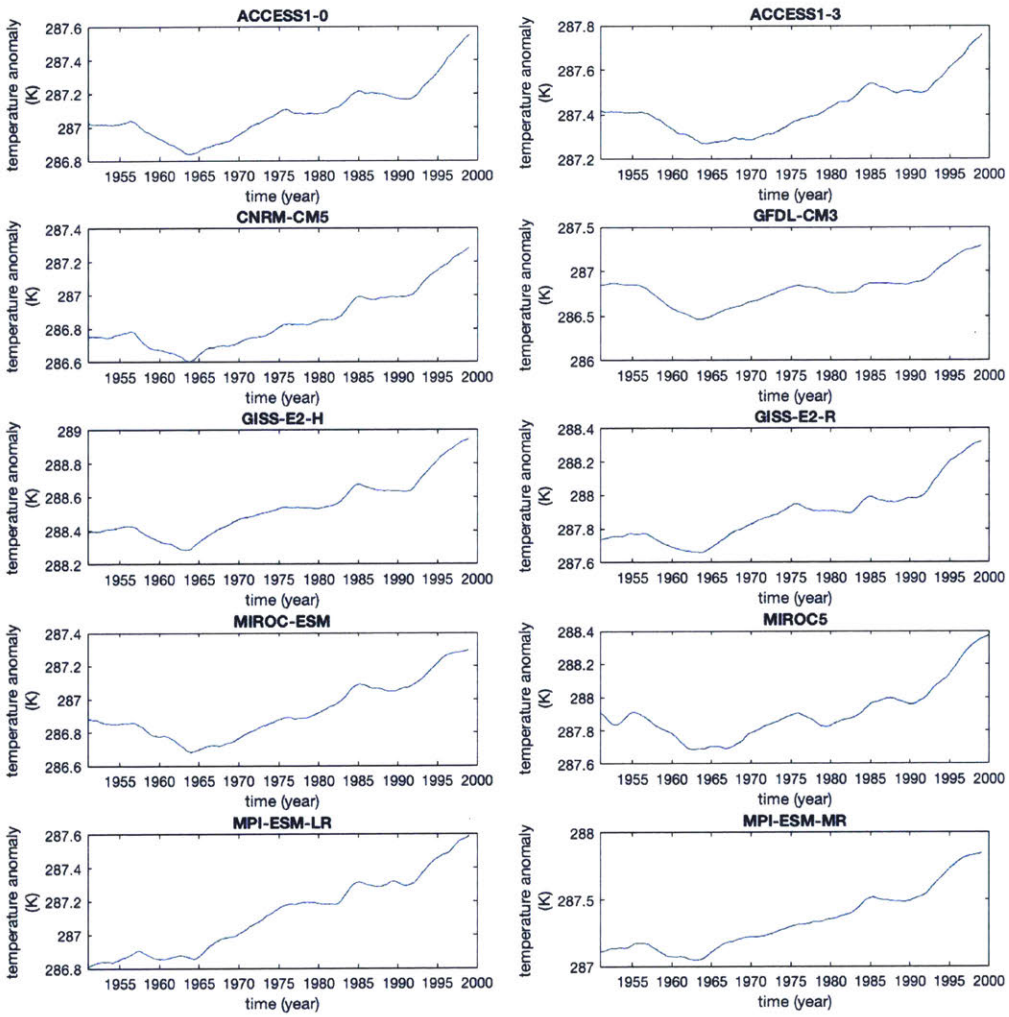

Figure 4-1. Global mean, 7-year running mean surface temperature from CMIP5 models from 1951 – 1999.

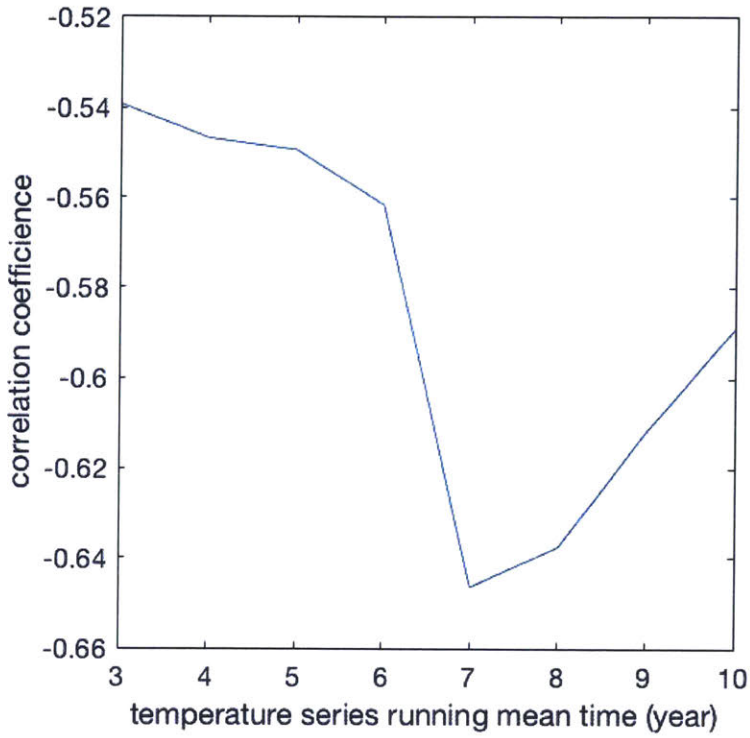

Figure 4-2. The correlation coefficient between the regression coefficient of surface temperature response to volcanic forcing and the model's respective transient climate response versus the number of running mean years used for running mean temperature series. The maximum negative correlation is for a 7-year running mean series.

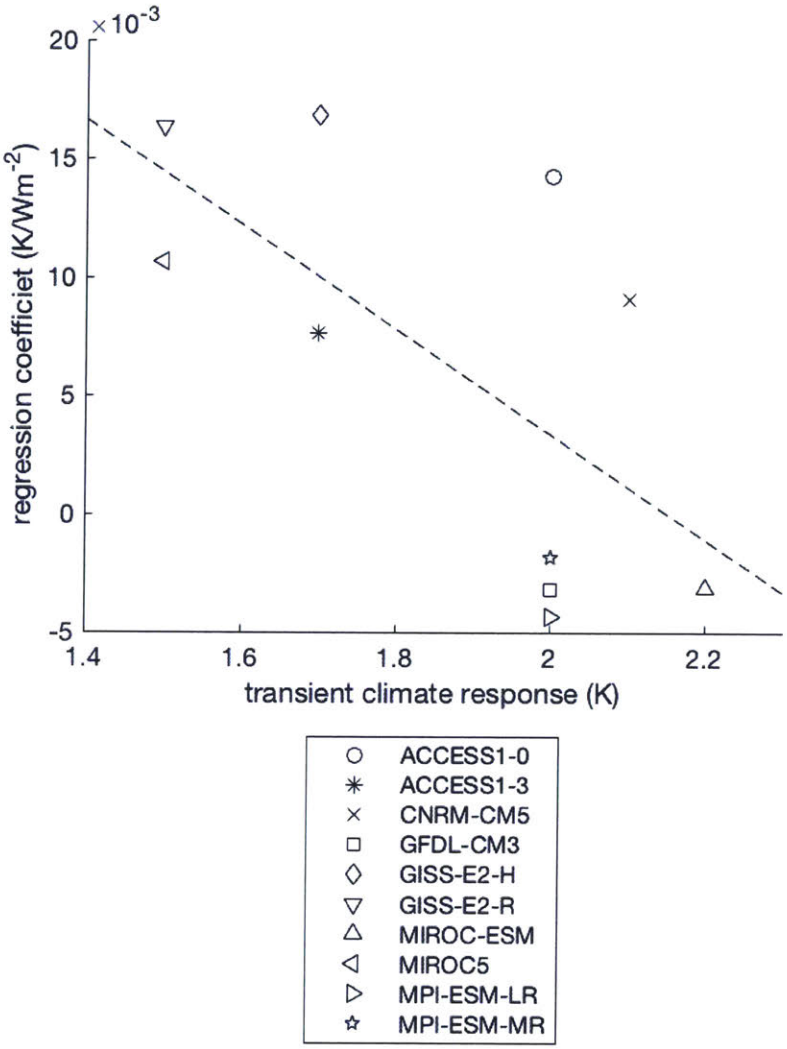

Figure 4-3. 7-year running mean series' regression coefficient of surface temperature response to volcanic forcing versus transient climate response. The dashed line shows the best fit line of this data set. The correlation coefficient is -0.65 with p = 0.04.

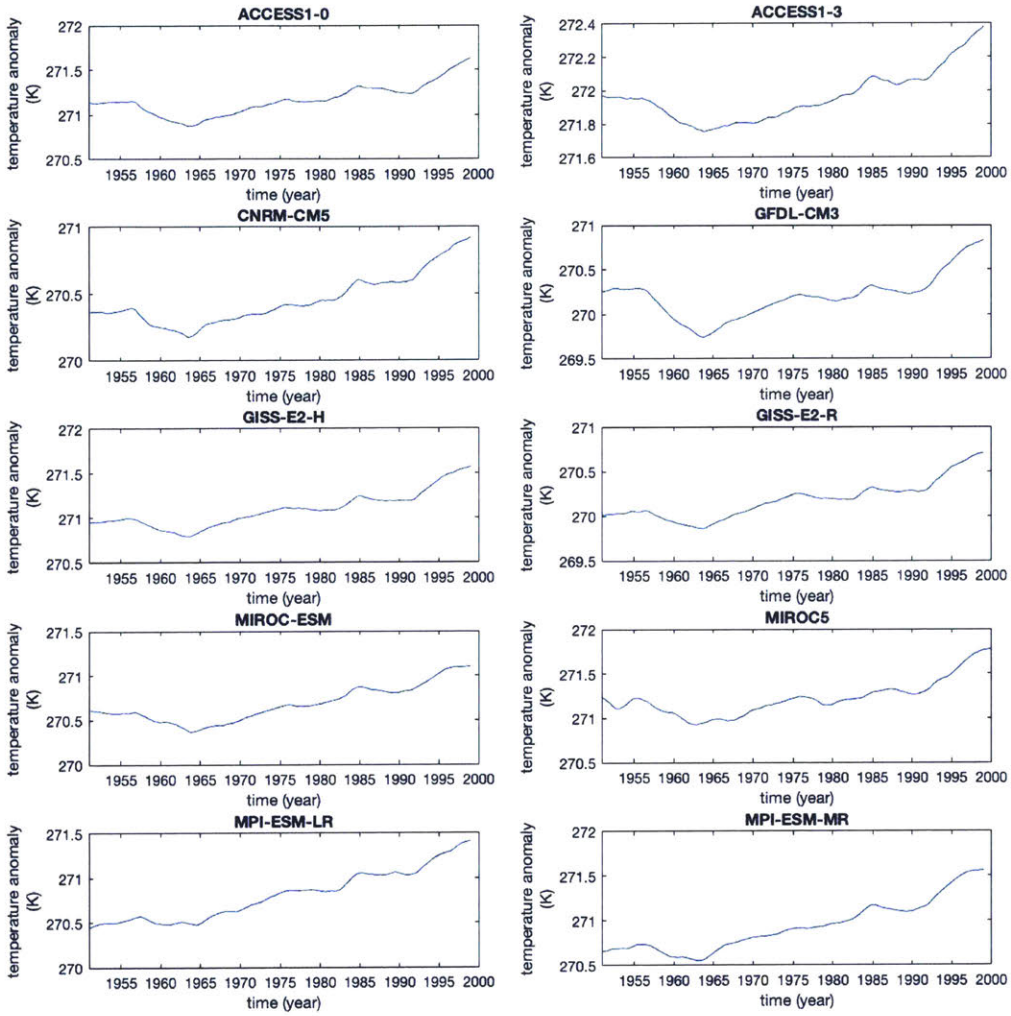

Figure 4-4. Global mean, 7-year running mean lower-troposphere temperature from CMIP5 models from 1951 – 1999.

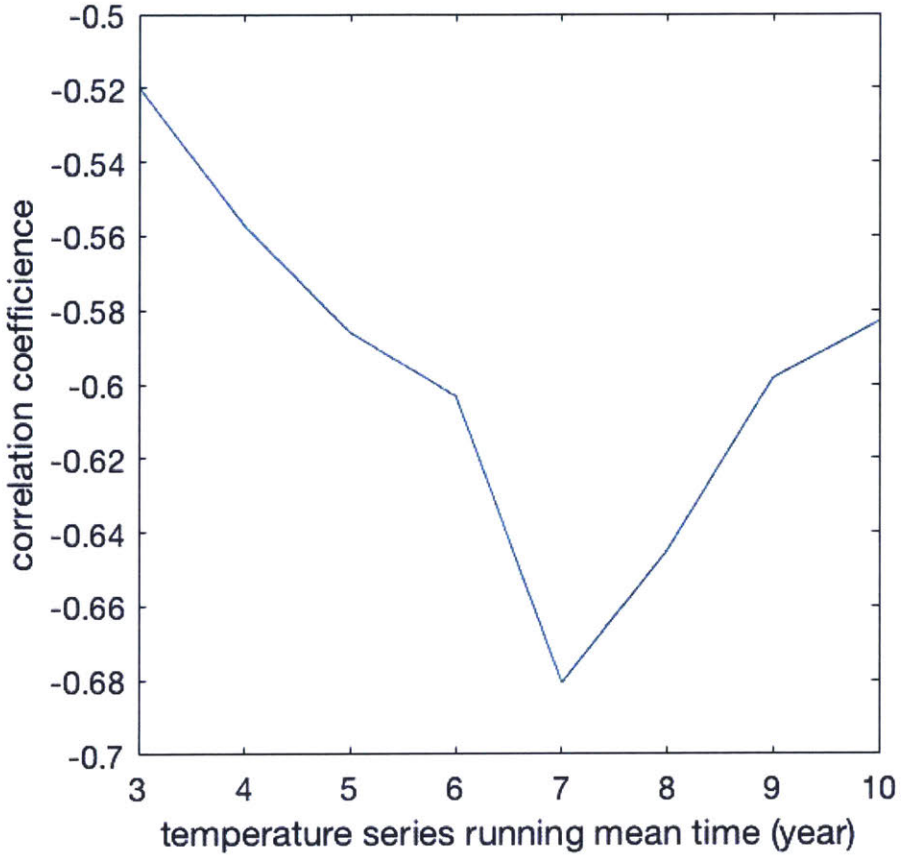

Figure 4-5. The correlation between the regression coefficient of lower-troposphere temperature response to volcanic forcing and the model's respective transient climate response versus the number of running mean years used for running mean temperature series. The maximum negative correlation is for the 7-year running mean series.

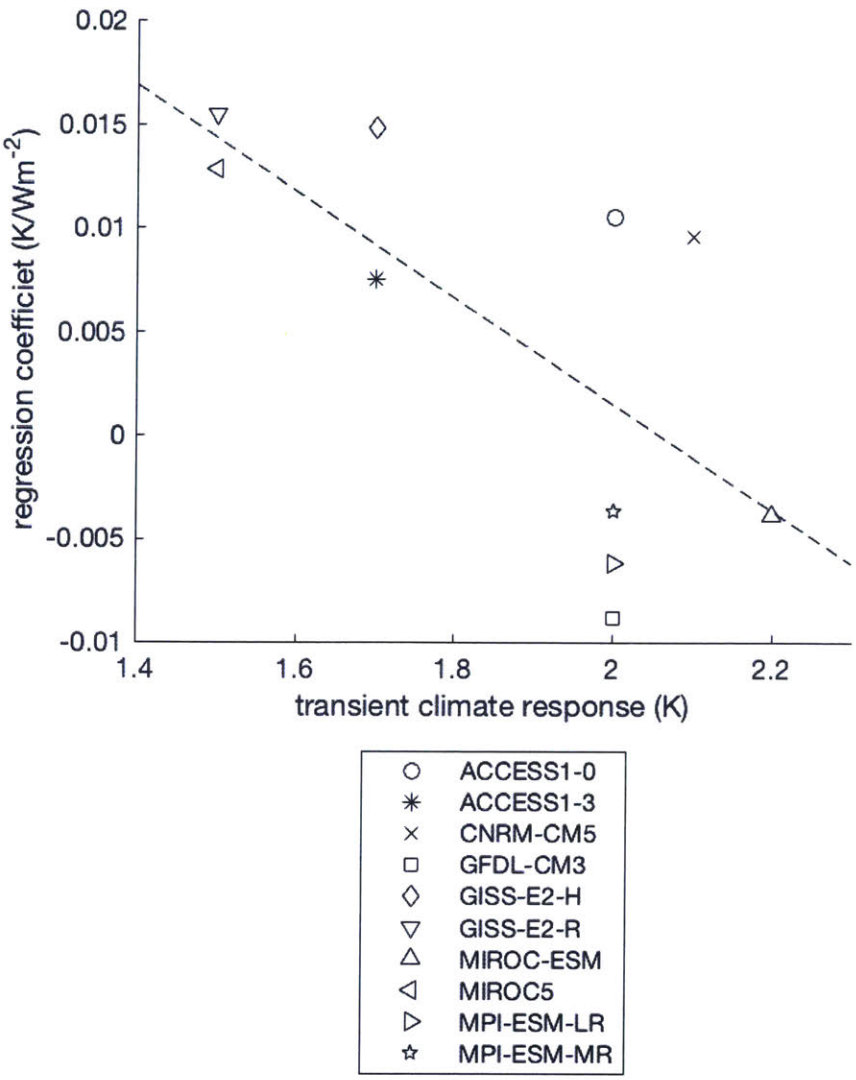

Figure 4-6. 7-year running mean series' regression coefficient of lower-troposphere temperature response to volcanic forcing versus transient climate response. The dashed line shows the best fit line of this data set. The correlation coefficient is -0.68 with p = 0.03.

Chapter 5

Discussion and Conclusion

5.1 Discussion and future work

We were unable to exactly reproduce Bender et al.'s result for CMIP3 models. However, we were able to reproduce the result for five out of ten models, and this was sufficient agreement to go forward to test the robustness for CMIP5 data. One possibility is that the CMIP3 data changed since the Bender et al. study, and in this sense it would be good to have access to the errata page for CMIP3.

In CMIP5 reflected shortwave anomalies series (figure 3-2), some short decreases in shortwave anomaly during the time it should be responding to volcanic forcing can be noticed. This is most likely because full-sky reflected shortwave was used in computing the series instead of clear-sky shortwave series. The presence of clouds in the model affected the reflected shortwave and disrupted its response to volcanic aerosols. However, all-sky out going shortwave data were intentionally chosen because they represent real world atmosphere better than theoretical clear-sky data. Nonetheless, the disrupted response contributed to the correlation between the scaled temperature perturbation and climate sensitivity being not statistically significant.

TCR and TLT were introduced in an attempt to improve the correlation using Bender et al.'s approach. Using TCR or TLT in the calculation improved the correlation. However, the combination of the two did not further improve the correlation as shown in table 3.

The regression approach succeeded in giving a tighter constraint for transient climate response, with a significant correlation coefficient of -0.65 and $p = 0.04$ for surface temperature. The correlation coefficients produced for running-mean times of 4 to 10-years show smooth variation with running mean time, suggesting that the peak correlations at 7 years is unlikely to be random. The correlation may be able to be improved further by finding the best number of years for each models' running mean, because each model might have a different ocean heat flux, resulting in a different lag in

temperature response to volcanoes. The running-mean time for each model may be approximated from the time it takes sea surface temperature to reach equilibrium after instant cooling from volcanic forcing.

Table 5.1. Correlation coefficient and p-value from each approach

Approach	Experiment	Correlation Coefficient (r)	p-Value
Bender et al.'s	CMIP3 TAS vs. ECS	-0.44	0.23
	CMIP5 TAS vs. ECS	-0.22	0.63
	CMIP5 TAS vs. TCR	-0.38	0.28
	CMIP5 TLT vs. ECS	-0.43	0.29
	CMIP5 TLT vs. TCR	-0.40	0.25
Regression	CMIP5 TAS vs. TCR	-0.65	0.04
	CMIP5 TLT vs. TCR	-0.68	0.03

The future may explore the use of transient climate response for estimating climate sensitivity calculated from lower-troposphere temperature an alternative to equilibrium climate sensitivity. Its shorter time-scale help tighten the constraint as well as makes it more useful for policy making. Transient climate response of even shorter time-scale may be explored as well.

5.2 Conclusion

We find that Bender et al.'s approach to constraining climate sensitivity is not robust with CMIP5 model data. However, the link between volcanic response and climate sensitivity improved when using transient climate response instead of equilibrium climate sensitivity and lower-troposphere temperature instead of surface air temperature. The regression approach can be calculated using different period of time to calculate running mean series. We find that the best correlation is produced from 7-year running mean series.

Bibliography

Ammann, C. M., Meehl, G. A., Washington, W. M., & Zender, C. S. (2003). A monthly and latitudinally varying volcanic forcing dataset in simulations of 20th century climate. *Geophysical Research Letters*, *30*(12).

Bender, F. A. M., Ekman, A. M., & Rodhe, H. (2010). Response to the eruption of Mount Pinatubo in relation to climate sensitivity in the CMIP3 models. *Climate dynamics*, 35(5), 875-886.

Boer, G. J., Stowasser, M., & Hamilton, K. (2007). Inferring climate sensitivity from volcanic events. *Climate dynamics*, *28*(5), 481-502.

Church, J. A., White, N. J., & Arblaster, J. M. (2005). Significant decadal-scale impact of volcanic eruptions on sea level and ocean heat content. *Nature*, *438*(7064), 74-77.

Foster, G., & Rahmstorf, S. (2011). Global temperature evolution 1979–2010. *Environmental Research Letters*, 6(4), 044022.

IPCC (2001). Climate Change 2001: *the scientific basis*. Contribution of Working Group I to the Third Assessment Report of the Intergovernmental Panel on Climate Change. In: Houghton JT, Ding Y, Griggs DJ, Noguer M, van der Linden PJ, Dai X, Maskell K, Johnson CA (eds) Cambridge University Press, Cambridge, and New York, p 881

IPCC (2013). Climate Change 2013: *The Physical Science Basis*. Contribution of Working Group I to the Fifth Assessment Report of the Intergovernmental panel on Climate Change [Stocker, T.F., D. Qin, G.-K. Plattner, M. Tignor, S.K. Allen, J. Boschung, A. Nauels, Y. Xia, V. Bex and P.M. Midgley (eds.)]. Cambridge University Press, Cambridge, United Kingdom and New York, NY, USA, 1535 pp, doi:10.1017/CBO9781107415324.

Lindzen, R. S., & Giannitsis, C. (1998). On the climatic implications of volcanic cooling. *Journal of Geophysical Research: Atmospheres*, *103*(D6), 5929-5941.

Rampino, M. R., & Self, S. (1984). Sulphur-rich volcanic eruptions and stratospheric aerosols. *Nature*, 310, 677-679.

Sato, M., Hansen, J. E., McCormick, M. P., & Pollack, J. B. (1993). Stratospheric aerosol optical depths, 1850–1990. *Journal of Geophysical Research: Atmospheres*, *98*(D12), 22987-22994.

Soden BJ, Wetherald RT, Stenchikov GL, Robock A (2002) Global cooling after the eruption of Mount Pinatubo: a test of climate feedback by water vapour. *Science* 296:727–730

Wigley, T. M. L., Ammann, C. M., Santer, B. D., & Raper, S. C. (2005). Effect of climate sensitivity on the response to volcanic forcing. *Journal of Geophysical Research: Atmospheres*, *110*(D9).

Wigley, T. M. L., Ammann, C. M., Santer, B. D., & Taylor, K. E. (2005). Comment on "Climate forcing by the volcanic eruption of Mount Pinatubo" by David H. Douglass and Robert S. Knox. *Geophysical research letters*, *32*(20).

Yokohata, T., Emori, S., Nozawa, T., Tsushima, Y., Ogura, T., & Kimoto, M. (2005). Climate response to volcanic forcing: Validation of climate sensitivity of a coupled atmosphere-ocean general circulation model. *Geophysical Research Letters*, *32*(21).